Macromolecules

pubs.acs.org/Macromolecules Article

Formaldehyde-Free Synthesis of Fully Bio-Based Multifunctional Bisbenzoxazine Resins from Natural Renewable Starting Materials

Mohamed Gamal Mohamed, Chia-Jung Li, Mo Aqib Raza Khan, Chih-Chuang Liaw, Kan Zhang,* and Shiao-Wei Kuo*

Cite This: *Macromolecules* 2022, 55, 3106–3115 Read Online

ACCESS | Metrics & More | Article Recommendations | Supporting Information

ABSTRACT: Although bio-based benzoxazines (BZs) have been explored widely as sustainable thermosetting resins, few high-performance BZs have been prepared completely from natural renewable resources. In this study we synthesized a fully bio-based multifunctional bisbenzoxazine (AP-fa-BZ) in high yield and purity from apigenin (AP), furfurylamine (fa), and benzaldehyde by using both solvent and solventless approaches. Fourier transform infrared (FTIR) spectroscopy, high-resolution mass spectrometry, and one- and two-dimensional nuclear magnetic resonance spectroscopy confirmed the chemical structure of AP-fa-BZ. We then used dynamic mechanical analysis, differential scanning calorimetry (DSC), thermogravimetric analysis, and *in situ* FTIR spectroscopy to examine the thermal characteristics of AP-fa-BZ before and after its ring-opening polymerization (ROP). DSC revealed that the temperature required for the formation of poly(AP-fa-BZ) through ROP (236.3 °C) was significantly lower than that of a typical 4-phenyl-3,4-dihydro-2*H*-1,3-benzoxazine (Pa-type) monomer due to the positive catalytic effect of the phenolic OH groups in the AP structure. After thermal polymerization at 250 °C, the resulting poly(AP-fa-BZ) possessed a high thermal decomposition temperature (T_{d10} = 395 °C), a high char yield (52 wt %), and a high glass transition temperature (T_g = 283 °C). Contact angle measurements revealed the tunable surface properties of AP-fa-BZ. Finally, the AP-fa-BZ resin functioned as an antibacterial agent against both *Staphylococcus aureus* and *Escherichia coli*.

INTRODUCTION

During the past three decades, syntheses of benzoxazine (BZ) monomers and their corresponding polybenzoxazines (PBZs) have developed rapidly fast in both academia and industry.[1] The chemical structure of a BZ monomer features a heterocyclic ring, containing both oxygen and nitrogen atoms, fused to a benzene ring. Its polymeric product can form through thermal ring-opening polymerization (ROP) without the need to add any potentially harmful catalysts (Scheme S1).[2−18] Holly and Cope prepared the first monofunctional BZ, 3,4-dihydro-2*H*-1,3-benzoxazine, through Mannich condensation.[19] Although the chemical structures of PBZs are similar to those of traditional phenolic resins, PBZs are generally prepared by using simple and self-catalyzed polymerization processes and display good heat resistance, high degradation and glass transition (T_g) temperatures, near-zero volumetric shrinkage during polymerization, excellent flame retardancy, good mechanical properties, low dielectric constants, water absorption properties, and variable surface free energies.[1,20−31] In addition, high flexibility in the molecular design of BZ resins allows a variety of physical and mechanical properties to be introduced into the resulting PBZ materials.[20−31] Moreover, the properties of PBZs lead to many potential applications in, for example, adsorbents, metal capture, energy storage, gas uptake, shape-memory and self-healing polymers, anticorrosion coatings, adhesives, and electronic materials.[32−45] The syntheses and characteristics of mono-, bi-, tri-, and tetrafunctional BZs have been investigated in detail by many research groups.[1,8,10,12,13,16,20,21] In general, monofunctionalized BZs tend to form linear polymers of relatively lower molecular weight, while bifunctional BZs form cross-linked macromolecules featuring more stable networks.[1]

Sustainable development is desired worldwide. To play its part, emerging research fields will have to find replacements for raw materials that are harmful to the environment and human body. For example, some natural renewable phenolic and amine derivatives are currently being used to synthesize BZ monomers from bio-based materials.[3,17,20,30] These renewable phenolic and amine compounds include sesamol, diphenolic acid, resveratrol, apigenin (AP), cardanol, guaiacol, coumarin, bisguaiacol-F, urushiol, vanillin, stearylamine, chitosan, furfur-

Received: February 26, 2022
Revised: March 20, 2022
Published: April 6, 2022

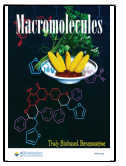

https://doi.org/10.1021/acs.macromol.2c00417
Macromolecules 2022, 55, 3106−3115

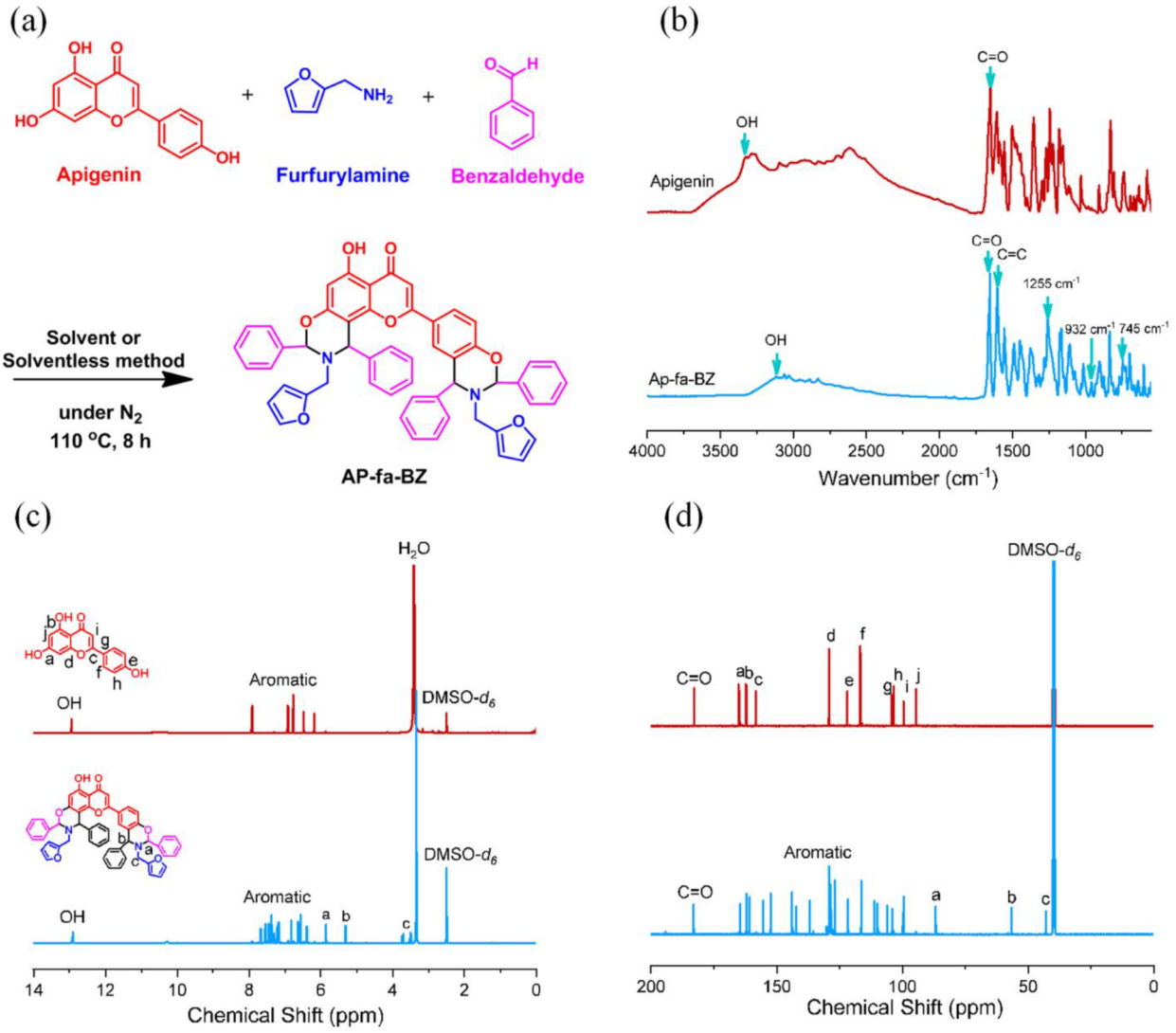

Figure 1. (a) Syntheses of the AP-fa-BZ monomer using both solvent and solventless methods. (b) FTIR, (c) ^{1}H NMR, and (d) ^{13}C NMR spectra of AP and AP-fa-BZ, measured at room temperature.

ylamine, and amines originating from rosin and isomannide.[46−53] The Liu and Zhang groups have reported that BZs originating from flavonoid precursors can provide high values of T_g due to additional cross-linking reactions occurring for the C═C units in the daidzein structure as well as cross-linked PBZ networks after polymerization.[54,55] AP is a bioflavonoid phenolic precursor that can be extracted from red wine, tea, apples, grapes, and parsley.[56,57] PBZ thermosets derived from AP have featured low polymerization temperatures and good thermal and mechanical properties due to intramolecular hydrogen bonding and additional cross-linked networks formed from C═C bonds.[58,59] Furthermore, an AP-derived BZ has been employed to prepare a porous organic polymer (POP) for application in energy storage.[18] Nevertheless, natural renewable formaldehyde has rarely been reported as a starting material for BZ synthesis, presumably because of the high cost of bio-based formaldehyde. Recently, oxazine ring-substituted fourth-generation BZ resins have been synthesized by using bio-based benzaldehyde.[60] For example, Ishida et al. prepared a fully bio-based monofunctional BZ monomer (S-fu-[2,4]benz) from the reaction of sesamol, furfurylamine, and benzaldehyde; its corresponding polymer possessed excellent thermal properties, as determined through thermogravimetric analysis (TGA).[61] Furthermore, the Lochab and Caillol groups discovered that BZs derived from benzaldehyde exhibited higher thermal stability but lower polymerization temperatures than those of monomers based on formaldehyde.[60,62]

In this study we synthesized a fully bio-based multifunctional bis-BZ (AP-fa-BZ) from the completely natural renewable resources AP, furfurylamine (fa), and benzaldehyde. Notably, benzaldehyde is a nontoxic compound, another salient feature of this newly designed BZ. Furthermore, we developed both solvent and solventless methods for the one-pot synthesis of this BZ through Mannich condensation (Figure 1a). We used Fourier transform infrared (FTIR) spectroscopy, high-resolution mass spectrometry (HRMS), and nuclear magnetic resonance (NMR) spectroscopy to confirm the chemical structure of AP-fa-BZ. Furthermore, we describe herein its thermal polymerization behavior, activation energy (E_a), thermal stability, glass transition temperature, tunable surface properties, and antibacterial activity toward *Staphylococcus aureus* and *Escherichia coli*.

https://doi.org/10.1021/acs.macromol.2c00417
Macromolecules 2022, 55, 3106−3115

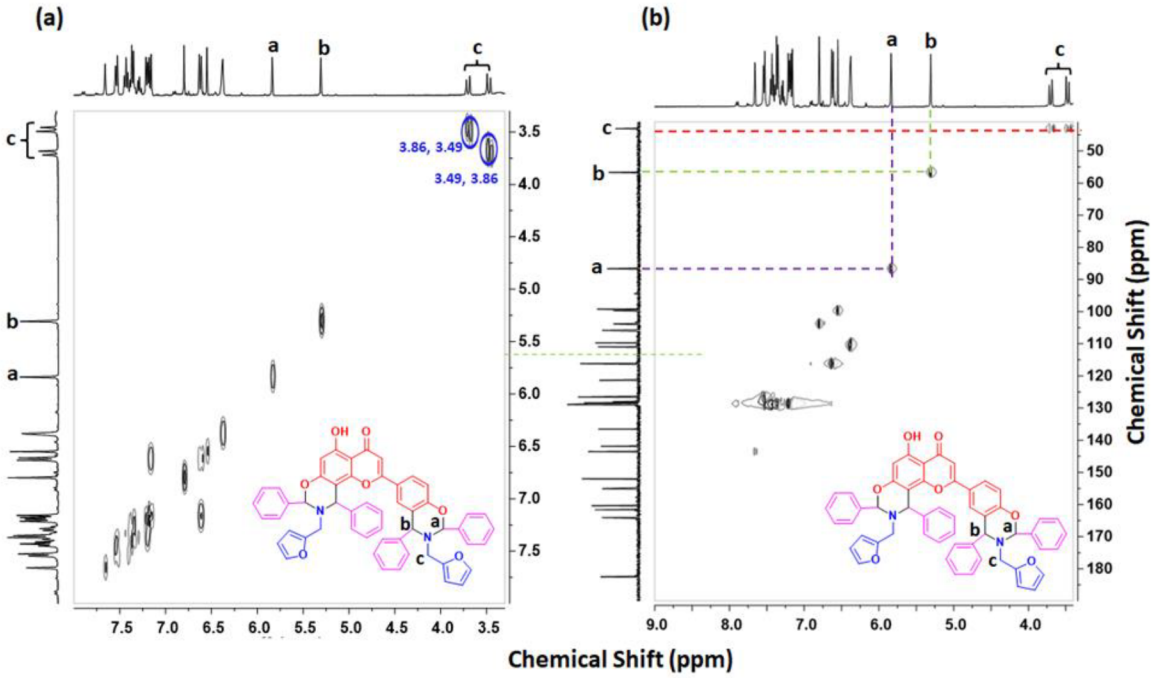

Figure 2. (a) $^{1}H-^{1}H$ COSY NMR and (b) $^{1}H-^{13}C$ HSQC NMR spectral analyses of AP-fa-BZ.

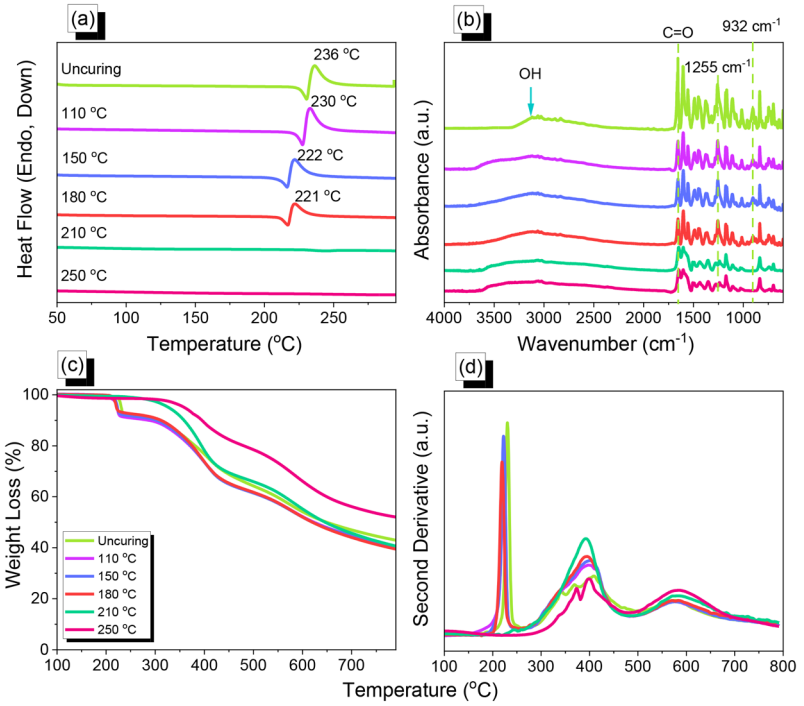

Figure 3. (a) DSC, (b) FTIR spectral, (c) TGA, and (d) second-derivative based on TGA analyses of AP-fa-BZ before and after thermal ROP at various temperatures.

EXPERIMENTAL SECTION

Materials. Apigenin (AP, $C_{15}H_{10}O_5$), benzaldehyde (C_7H_6O), and sodium hydroxide (NaOH) were purchased from Merck. Furfurylamine (C_5H_7NO) was purchased from Alfa Aesar. Dichloromethane (DCM), hexane, tetrahydrofuran (THF), ethyl acetate (EA), acetone, toluene, ethylene glycol (EG), diiodomethane (CH_2I_2), and methanol (CH_3OH) were purchased from J. T. Baker.

Synthesis of AP-fa-BZ through the Solvent Method. A solution of AP (0.80 g, 1.0 mmol), furfurylamine (0.78 mL, 3.0 mmol), and benzaldehyde (1.8 mL, 6.0 mmol) in toluene (50 mL) and ethanol (25 mL) was stirred under reflux at 110 °C for 6 h. After cooling, DCM was added to precipitate a beige powder. This beige solid was stirred in NaOH solution (1 N) at 25 °C and then the solid was filtered off and washed with H_2O until the pH reached 7. Finally, the solid was then recrystallized from a mixture of acetone and toluene (1:1), affording a beige solid (80%).

Synthesis of AP-fa-BZ through the Solventless Method. A mixture of AP (0.80 g, 1.0 mmol), furfurylamine (0.78 mL, 3.0 mmol), and benzaldehyde (1.8 mL, 6.0 mmol) was stirred at 110 °C for 6 h. After cooling, DCM was added to afford a beige powder. This

https://doi.org/10.1021/acs.macromol.2c00417
Macromolecules 2022, 55, 3106−3115

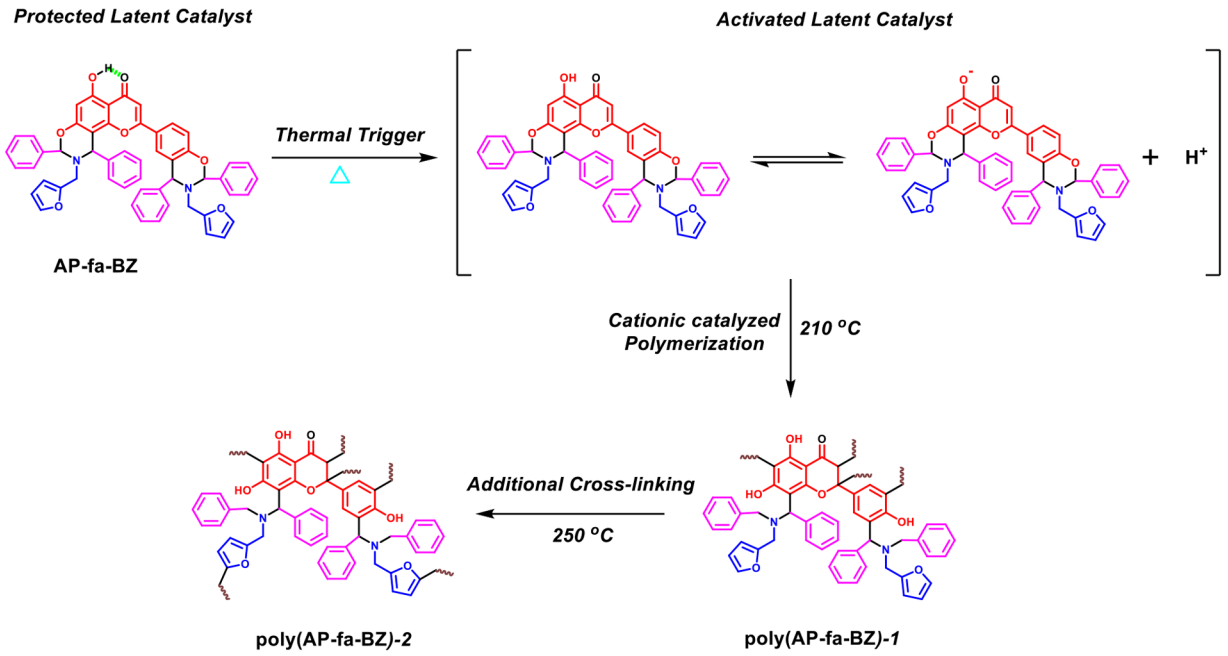

Figure 4. Suggested mechanism of the transformation of AP-fa-BZ after ROP.

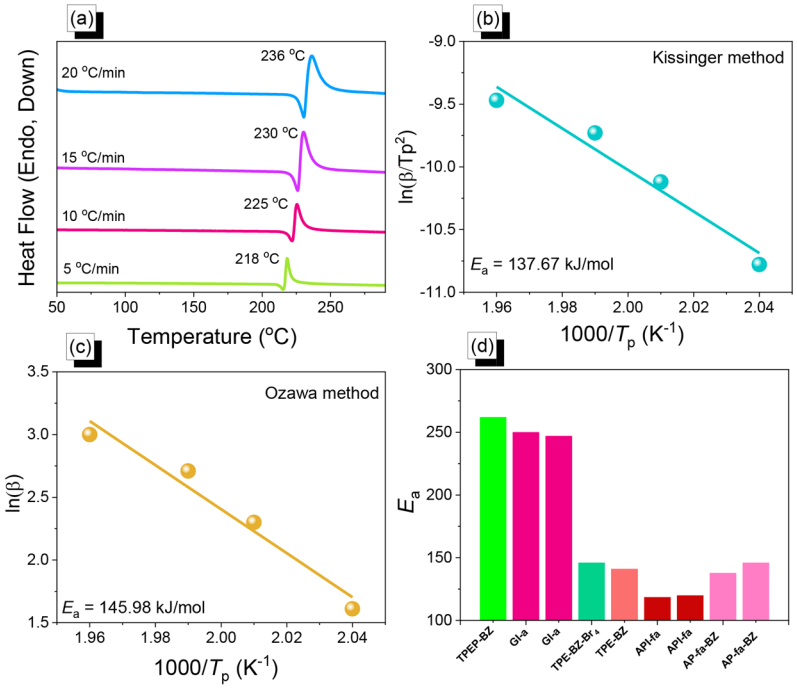

Figure 5. (a) Kinetic thermal curing behavior of AP-fa-BZ at various heating rates (through DSC measurements. (b, c) Calculations of the values of E_a of AP-fa-BZ by using the (b) Kissinger and (c) Ozawa methods. (d) Values of E_a of AP-fa-BZ and other BZ materials.

beige solid was stirred in NaOH solution (1 N) at 25 °C, and then the solid was filtered off and washed with H_2O until the pH reached 7. Then, the solid was then recrystallized from a mixture of acetone and toluene (1:1) afforded a beige solid (83%). FTIR (cm^{-1}): 3328 (phenolic OH), 1657 (C═O), 1601, 1552, 1380, 1316, 1255 (symmetric stretching vibrations of the Ar−O−C unit), 1165, 1071, 932 (oxazine ring-related band), 998, 871, 833, 738. ^{1}H NMR (DMSO-d_6, ppm): 12.87, 5.83, 5.31, 3.84, 3.69. ^{13}C NMR (DMSO-d_6, ppm): 183.58, 164.57−98.53, 86.51, 56.95, 42.49.

Preparation of Poly(AP-fa-BZ) via ROP of AP-fa-BZ. A desired amount of AP-fa-BZ was placed in an aluminum pan in an oven, and then the temperature was increased from 110 to 250 °C at a heating rate of 5 °C min^{-1} over 2 h. A black product was obtained after curing at 210 and 250 °C, indicating the formation of poly(AP-fa-BZ).

Preparation of AP-fa-BZ Monomer and Poly(AP-fa-BZ) for Contact Angle Measurements. A solution of AP-fa-BZ monomer (3 wt %) in a definite amount of THF was placed on glass and dried in an oven at 50 °C for 24 h. Contact angles (CAs) were then measured for the uncured AP-fa-BZ and for the cured samples after thermal treatment at various temperatures (110, 150, 180, 210, and 250 °C). Three CA measurements were averaged for each type of film by using H_2O, ethylene glycol (EG), and methylene iodide (CH_2I_2) as standards.

https://doi.org/10.1021/acs.macromol.2c00417
Macromolecules 2022, 55, 3106−3115

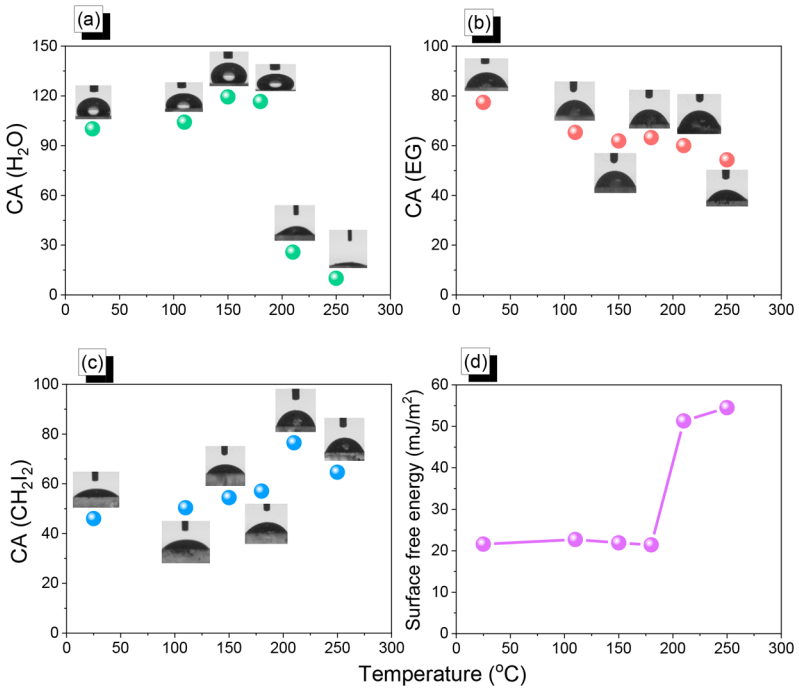

Figure 6. (a–c) CAs of AP-fa-BZ before and after thermal curing: (a) DI water, (b) EG, and (c) CH_2CI_2. (d) Surface free energies of AP-fa-BZ after applying various curing temperatures based on CA analyses.

Preparation of AP-fa-BZ and Poly(AP-fa-BZ) for Antibacterial Activity. The bacterial cultures were inoculated in brain heart infusion (BHI) agar at 25 °C for 24 h and then diluted with cation-adjusted Mueller–Hinton broth (CAMHB) to adjust the turbidity approximately to the standard McFarland 0.5 (2×10^8 CFU mL^{-1}). The bacterial suspension was then further diluted by 200 times with CAMHB broth to achieve an initial loading of 1×10^6 CFU mL^{-1}. Both the monomer and polymer were redissolved in DMSO. The bacterial suspension (195 μL) and tested compound solution (5 μL) at two concentrations (125 and 62.5 μg mL^{-1}) were added to each well of a 96-well plate and incubated for 24 h at 25 °C. Finally, the tested 96-well plate was examined by using an ELISA reader at OD_{600} to evaluate the minimum inhibitory concentrations (MICs). All data (treated and untreated bacteria) were measured in triplicate. Samples of the bacteria without AP-fa-BZ and Poly(AP-fa-BZ) were used as negative controls in the tests.

RESULTS AND DISCUSSION

Synthesis and Characterization of AP-fa-BZ Monomer. Large numbers of BZ monomers and their corresponding polymers (after thermal curing polymerization) have been examined for the flexible and simple molecular design of BZ resins.[1] In this study, we attempted the synthesis of a fully bio-based bis-BZ derived from AP as the bio-based phenol source, fa as the amine source, and benzaldehyde. Initially, we tested DMSO as the solvent for the Mannich condensation, but this approach produced BZ monomers in low yield and with many unidentified impurities. In contrast, the AP-fa-BZ monomer was obtained in high yield and with excellent purity when using a one-pot solvent (toluene/ethanol) or solventless method for the Mannich condensation of AP, fa, and benzaldehyde at 110 °C for 6 h. These synthetic methods for producing AP-fa-BZ are simple and environmentally friendly, with no release of toxic waste or polluting materials. The presence of the oxazine ring in the AP-fa-BZ structure was confirmed by using ^{1}H, ^{13}C, and 2D NMR spectroscopy, FTIR spectroscopy, and differential scanning calorimetry (DSC). The FTIR spectra of AP and AP-fa-BZ (Figure 1b) featured absorption bands centered at 1655 and 1501 cm^{-1} representing their C=O and C=C stretching vibrations. The spectrum of AP-fa-BZ contained absorption bands at 1255 and 1071 cm^{-1} for the symmetric and asymmetric stretching vibrations, respectively, of the Ar–O–C unit in the oxazine ring. In addition, the presence of free phenolic OH in AP-fa-BZ can be observed at 3328 cm^{-1}. The asymmetric stretching modes of the C–N–C bond in the oxazine ring of the BZ ring appeared at 1380 and 1165 cm^{-1}. Moreover, the characteristic oxazine ring-related band occurred at 932 cm^{-1}. The incorporation of the furan moiety into AP-fa-BZ was confirmed by typical bands in the FTIR spectrum at 1601, 1380, 833, and 745 cm^{-1}. We compared the ^{1}H and ^{13}C NMR spectra of AP and the newly synthesized AP-fa-BZ as solutions in DMSO-d_6. The ^{1}H NMR spectrum in Figure 1c reveal signals at 12.94 ppm and in the range 7.89–6.18 ppm for the free phenolic OH groups and aromatic rings of AP. The ^{13}C NMR spectrum of AP (Figure 1d) featured signals centered at 182.04 ppm and in the range 165.55–93.50 ppm representing the carbonyl (C=O) group in the pyrone structure and the aromatic units, respectively. Figure 1c reveals

Table 1. Surface Properties Analysis of AP-fa-BZ before and after Thermal Treatments

	contact angle (deg)			
AP-fa-BZ	DI water	ethylene glycol	diiodomethane	surface free energy (mJ/m^2)
uncuring	100.1	77.4	46.0	21.6
110 °C	104.1	65.3	50.4	22.7
150 °C	119.3	61.8	54.5	21.9
180 °C	116.6	63.2	57.1	21.4
210 °C	25.8	60.0	76.5	51.3
250 °C	12.0	54.3	64.6	54.5

https://doi.org/10.1021/acs.macromol.2c00417
Macromolecules 2022, 55, 3106–3115

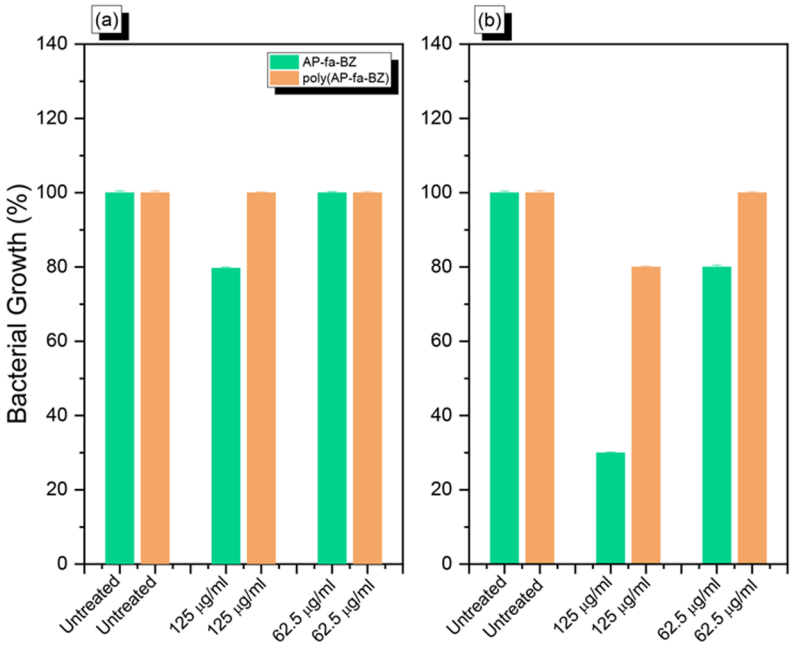

Figure 7. Antibacterial activity of AP-fa-BZ and its corresponding polymer against (a) *Escherichia coli* and (b) *Staphylococcus aureus* determined by using the broth microdilution method.

that the main ^{1}H NMR spectral signals of AP-fa-BZ were located at 12.87 and 3.69/3.84 ppm, corresponding to the protons of the OH group and furan moiety, respectively. The ^{1}H NMR signal for the FurCH_2N unit of AP-fa-BZ appeared as two separated peaks, consistent with the expected magnetic nonequivalence of these geminal protons. The ^{1}H−^{1}H COSY NMR spectrum of AP-fa-BZ in Figure 2a confirmed the coupling of these protons in the FurCH_2N unit. Furthermore, signals appeared at 5.83 and 5.31 ppm for the OCHN and ArCHN protons, respectively, in the oxazine ring of AP-fa-BZ. The ^{13}C NMR spectrum of AP-fa-BZ (Figure 1d) confirmed the presence of C═O (183.58 ppm), OCHN (86.51 ppm), ArCHN (56.95 ppm), and furan (42.49 ppm) units in the AP-fa-BZ structure. The ^{1}H−^{13}C HSQC NMR spectrum of AP-fa-BZ in Figure 2b revealed that both of the geminal protons in the FurCH_2N unit were correlated to carbon atom (c), with the proton of the OCHN unit (a) directly correlated to the carbon atom (a) and the proton of the ArCHN unit (b) correlated to the carbon atom (a) in the oxazine ring. Thus, the spectra in Figure 1 allowed identification of all of the signals of the protons and carbon nuclei of AP and AP-fa-BZ. HRMS confirmed the successful synthesis of AP-fa-BZ, and its purity (Figure S1). A peak appeared at m/z 817.29, equal to the theoretical molecular weight of AP-fa-BZ ($C_{53}H_{41}N_2O_7$). Furthermore, the ^{1}H NMR spectrum of the AP-fa-BZ monomer recorded after being stored for more than 5 months (Figure S2) featured all of the expected signals, confirming that our new BZ monomer possessed excellent stability.

Thermal Behavior of AP-fa-BZ Monomer. We employed DSC, *in situ* FTIR spectroscopy, and TGA to investigate the thermal ROP behavior of AP-fa-BZ (Figure 3). The DSC thermogram of the uncured AP-fa-BZ in Figure 3a revealed two visible thermal events: a sharp endothermic peak and a maximum exothermic curing peak. The first thermal event, at the lower temperature of 230 °C, represents the melting temperature of the AP-fa-BZ crystal. The high melting point of the AP-fa-BZ monomer due to high content of aromatic rings and rigidity in a single molecule. The second event, at 236 °C, can be attributed mainly to opening of the oxazine ring in AP-fa-BZ and the formation of its polymeric product, poly(AP-fa-BZ), at this higher temperature. Notably, the sharp and symmetric melting peak of AP-fa-BZ confirms its high purity; as a result, we infer that any effect of impurities on the induced temperature for ROP of AP-fa-BZ was negligible. Because the onset of the curing peak of AP-fa-BZ overlapped with its melting point, the polymerization of AP-fa-BZ must have occurred immediately upon the melting of AP-fa-BZ. Furthermore, after thermal treatment of AP-fa-BZ at 110 °C, both the maximum exothermic and melting point peaks shifted to lower temperatures (233 and 226 °C, respectively). This behavior indicated that the crystal form of AP-fa-BZ had changed after thermal treatment, with the structural transformation also affecting its ROP process. In addition, after thermal treatment at 150 and 180 °C, the sharp endothermic peaks shifted to temperatures of 216 and 214 °C, respectively, and the exothermic peaks to 222 and 221 °C, respectively. The continued decreases in the melting and curing temperatures of AP-fa-BZ at these two temperatures are indicative of a remaining thermal latent catalytic effect. When the temperature of thermal treatment increased to 210 and 250 °C, however, the exothermic peak and the peak for the melting point disappeared completely. To monitor the structural transformations of AP-fa-BZ and its corresponding polymers at these various thermal curing temperatures, we performed *in situ* FTIR spectral measurements (Figure 3b). When we increased the thermal curing temperature from 110 to 180 °C, the characteristic absorption signals of AP-fa-BZ at 1656 cm^{-1} (C═O groups in the AP structure), 1255 cm^{-1} (C−O−C symmetric stretching), 1560 cm^{-1} (C═C in-plane-stretching), and 932 cm^{-1} (oxazine ring) were still present but with decreasing intensities. The characteristic bands of AP-fa-BZ were absent after thermal curing at 210 and 250 °C, suggesting that the oxazine ring in the BZ moiety had undergone ROP to form a cross-linked and more thermally stable poly(AP-fa-BZ).

https://doi.org/10.1021/acs.macromol.2c00417
Macromolecules 2022, 55, 3106−3115

Figure 4 provides a suggested mechanism for the transformation of AP-fa-BZ during the ROP process, according to the DSC and FTIR spectral data. The latent catalytic features of AP-fa-BZ presumably arose from a stable intramolecular hydrogen bonding system, with these noncovalent interactions acting as a protecting group under ambient conditions. To prove this concept, we performed a ^{1}H NMR spectral analysis of AP-fa-BZ in $CDCl_3$ (Figure S3). Initially, the signal of the phenolic OH group was a sharp singlet with acceptable integration value, suggesting that the catalytic and activating effect of the OH group was subdued through stable intramolecular hydrogen bonding with C═O groups. When the temperature increased to reach the melting point of AP-fa-BZ, the intramolecular hydrogen bonding became sufficiently weak to allow the phenolic OH group to interact with the oxazine ring. At 210 °C, partial polymerization of AP-fa-BZ occurred to form poly(AP-fa-BZ)-1 through ROP of the oxazine ring and additional C═C polymerization of the benzopyrone ring. Finally, poly(AP-fa-BZ)-1 underwent further additional cross-linking polymerization of the furan moieties at a higher temperature of 260 °C, affording poly(AP-fa-BZ)-2 as a highly cross-linked network.

We recorded TGA profiles to investigate the thermal stability (in terms of the temperature for 10 wt % decomposition (T_{d10}) and char yield) of AP-fa-BZ before and after its thermal curing polymerization at various temperatures (Figure 3c and Table S1). The value of T_{d10} and the char yield of the uncured BZ monomer were 297 °C and 43 wt %, respectively. Interestingly, after thermal treatment at 110 °C, the thermal stability of newly obtained bio-based BZ monomer (287 °C and 41 wt %) had decreased dramatically relative to that of the uncured sample, consistent with the loss in the crystallinity of AP-fa-BZ observed by using DSC (Figure 3a). After curing at 150 and 180 °C, the values of T_{d10} increased to 302 and 312 °C, respectively. As expected, thermal treatment at 210 and 250 °C caused both the degradation temperature and char yield to increase (to 359 °C/40 wt % and 400 °C/52 wt %, respectively) because the presence of the furan moieties and more aromatic carbon atoms from the AP unit,[63] as well as the complete ROP of the BZ monomer, resulted in the formation of a more stable structure that displayed improved thermal stability. Based on the Van Krevelan and Hoftyzer equation,[59,61] the limiting oxygen indices (LOI) of AP-fa-BZ and its polymers obtained after curing at 210 and 250 °C were 34.7%, 37.1%, and 38.3%, respectively; these values are above the threshold of 26%, suggesting that our new materials could be considered as self-extinguishable and antiflammable. In addition, as revealed in Figures 3c and 3d, the curing peak of AP-fa-BZ near 230 °C was completely absent after thermal curing polymerization at 210 and 250 °C, consistent with the FTIR spectral and DSC data. We used dynamic mechanical analysis (DMA) to measure the values of T_g of poly(AP-fa-BZ) (Figure S4). We observed a high value of T_g, with a shoulder peak, at 283 °C, arising from the combination of two different cross-linking densities that originated from the polymerization of the BZ and furan units at elevated temperatures.

We also investigated the activation energy (E_a) of AP-fa-BZ through DSC measurements performed at heating rates of 5, 10, 15, and 20 °C min^{-1} (Figure 5a). We calculated the values of E_a using the well-established Kissinger and Ozawa methods,[64,65] applying the following equations:

$$\ln\left(\frac{\beta}{T_p^2}\right) = \ln\left(\frac{AR}{E_a}\right) - \frac{E_a}{RT_p} \quad \text{Kissinger equation} \tag{1}$$

$$\ln \beta = -1.052\frac{E_a}{RT_p} + C \quad \text{modified Ozawa equation} \tag{2}$$

where β is the heating rate, A is the pre-exponential factor, T_p is the temperature at the exothermic peak maximum, R is the gas constant, and C is a constant. When the heating rate was 20 °C min^{-1}, the polymerization temperature of AP-fa-BZ was 236 °C; at 15, 10, and 5 °C min^{-1}, the polymerization temperatures of AP-fa-BZ were 230, 225, and 218 °C, respectively (Figure 5a), thereby providing values of E_a of AP-fa-BZ of 137.67 kJ mol^{-1} through the Kissinger theory (Figure 5b) and 145.98 kJ mol^{-1} through the Ozawa method (Figure 5c). Notably, previously reported values of E_a for the *ortho*-BZ monomer were 247 and 250 kJ mol^{-1} when calculated by using the Kissinger and Ozawa methods, respectively. This kinetic analysis confirmed that when compared with the traditional BZ structure, our newly designed bio-based AP-fa-BZ could more readily undergo ROP, without consuming too much energy, because of the latent catalytic group present in its BZ structure. In addition, the values of E_a for AP-fa-BZ were also lower than those of the previously reported BZ monomers TPEP-BZ,[16] GI-a,[66] TPE-BZ-Br$_4$,[13] and TPE-BZ[21] as well as that of API-fa.[59] Furthermore, we found that thermal curing at 110 °C resulted in values of E_a for AP-fa-BZ of 34.18 kJ mol^{-1} when applying Kissinger theory (Figure S5) and 38.14 kJ mol^{-1} when applying the Ozawa method, possibly as a result of the partially polymerized structure.

Surface Properties of AP-fa-BZ Determined through CA Analyses. We used CA measurements to study the surface properties of AP-fa-BZ before and after ROP (Figure 6). The degree of hydrogen bonding and the number of coordination sites of the PBZ precursor had a great effect on surface free energy (γ_s). We used H_2O, EG, and CH_2I_2 to examine the values of γ_s of AP-fa-BZ and its resulting polymer films obtained after curing polymerizations at temperatures from 110 to 250 °C. Figure 6a reveals that tFigure 6he CAs of DI water on the films of uncured AP-fa-BZ (25 °C), and those cured at 110, 150, 180, 210, and 250 °C were 100.1, 104.1, 119.3, 116.6, 25.8, and 12°, respectively; for EG (Figure 6b), these values were 77.4, 65.3, 61.8, 63.2, 60.0, and 54.3°, respectively; and for CH_2I_2 (Figure 6c), they were 46.0, 50.4, 54.5, 57.1, 76.5, and 64.6°, respectively. The trends in these CAs of AP-fa-BZ are very different from those previously reported for PBZs.[21] We used the Owens, Wendt, Rabel, and Kaelble (OWRK) methods to evaluate the surface free energies of these AP-fa-BZ films (Table 1).[67,68] The values of γ_s of the uncured AP-fa-BZ and the sample cured at 180 °C were similar (21.6 and 21.4 mJ m^{-2}, respectively); the surface free energy of poly(AP-fa-BZ) increased, however, after thermal curing at 210 °C (51.3 mJ m^{-2}) and 250 °C (54.5 mJ m^{-2}) (Figure 6d). In a previous study, we found that typical BA-a- and BA-m-type BZs (Scheme S1b) possessed surface free energies of 19.2 and 16.4 mJ m^{-2}, respectively, after thermal curing at 210 °C because of strong intramolecular OH···N hydrogen bonding and a lower fraction of OH···O intermolecular hydrogen bonding.[5] In this study was synthesized the AP-fa-BZ monomer from benzaldehyde (and not from formaldehyde, as is typical), and it did not form strong intramolecular OH···N

https://doi.org/10.1021/acs.macromol.2c00417
Macromolecules 2022, 55, 3106−3115

hydrogen bonds; thus, it featured only OH···O intermolecular hydrogen bonding after thermal curing, as displayed in Figure 4. As a result, the poly(AP-fa-BZ) also exhibited only OH···O intermolecular hydrogen bonding, thereby inducing a relatively high surface free energies. Our analysis of surface free energies confirmed the unusual chemical structures of poly(AP-fa-BZ) after thermal polymerization.

Antibacterial Activity of AP-fa-BZ and Poly(AP-fa-BZ). We performed antibacterial assays according to previous reports, with a few modifications.[69,70] We determined the antibacterial activity of both the monomer and polymer against Gram-negative *Escherichia coli* and Gram-positive *Staphylococcus aureus* using the broth microdilution method. The antibacterial tests revealed that the AP-fa-BZ monomer possessed inhibitory activity toward both tested bacteria. In contrast, poly(AP-fa-BZ) displayed no inhibitory activity (Figure 7). To confirm the results of the microtiter broth antibacterial tests, we also evaluated AP-fa-BZ (monomer) and poly(AP-fa-BZ) for their antibacterial inhibitory potentials by using the paper disc method (Figures S6 and S7). Here, we used the zone of inhibition to distinguish the antibacterial performance. The results clearly manifested that AP-fa-BZ displayed good inhibitory activity toward both Gram-positive and Gram-negative bacteria, with poly(AP-fa-BZ) displaying no inhibitory activity. We suspect that the loss of antibacterial activity for poly(AP-fa-BZ) was due to degradation of some of the functional groups of AP-fa-BZ upon curing at elevated temperature.

CONCLUSION

We have used Mannich reactions to synthesize a multifunctional bis-BZ monomer (AP-fa-BZ) completely from natural and nontoxic renewable resources (AP, fa, and benzaldehyde). FTIR spectroscopy, HRMS, and 1D and 2D NMR spectroscopy confirmed the molecular structure of AP-fa-BZ. The formation of poly(AP-fa-BZ) required a lower temperature (ca. 236 °C) than that of the Pa-type BZ monomer (up to 260 °C), even though its precursor (AP-fa-BZ) exhibited excellent stability (long shelf life). Furthermore, poly(AP-fa-BZ) displayed high thermal stability (T_{d10} = 395 °C), a high char yield (52 wt %), a high glass transition temperature (283 °C), and a high surface free energy (54.5 mJ m^{-2}) after thermal polymerization at 250 °C. In addition, our new BZ resin could be used directly, without polymerization, as an antibacterial agent displaying excellent thermal stability.

ASSOCIATED CONTENT

Supporting Information

The Supporting Information is available free of charge at https://pubs.acs.org/doi/10.1021/acs.macromol.2c00417.

Characterization methods, preparation of P-a and B-a monomers and their corresponding polymers, thermal decomposition temperatures and char yield of the AP-fa-BZ monomer after various curing temperatures, FT-MS diagram of the AP-fa-BZ monomer, ^{1}H NMR spectrum of the AP-fa-BZ monomer after stored more than 5 months, DMA analysis of the AP-fa-BZ, recorded after thermal polymerization at 250 °C, calculation E_a of AP-fa-BZ by using the Kissinger and Ozawa methods after thermal treatment at 110 °C, antibacterial activity of AP-fa-BZ and poly(AP-fa-BZ) against *Escherichia coli* and *Staphylococcus aureus* by the paper disc method (PDF)

AUTHOR INFORMATION

Corresponding Authors

Kan Zhang − *Research School of Polymeric Materials, School of Materials Science and Engineering, Jiangsu University, Zhenjiang 212013, China;* orcid.org/0000-0003-4628-2704; Email: zhangkan@ujs.edu.cn

Shiao-Wei Kuo − *Department of Materials and Optoelectronic Science, Center for Functional Polymers and Supramolecular Materials, National Sun Yat-Sen University, Kaohsiung 804, Taiwan; Department of Medicinal and Applied Chemistry, Kaohsiung Medical University, Kaohsiung 807, Taiwan;* orcid.org/0000-0002-4306-7171; Email: kuosw@faculty.nsysu.edu.tw

Authors

Mohamed Gamal Mohamed − *Department of Materials and Optoelectronic Science, Center for Functional Polymers and Supramolecular Materials, National Sun Yat-Sen University, Kaohsiung 804, Taiwan; Chemistry Department of Chemistry, Faculty of Science, Assiut University, Assiut 71516, Egypt;* orcid.org/0000-0003-0301-8372

Chia-Jung Li − *Department of Materials and Optoelectronic Science, Center for Functional Polymers and Supramolecular Materials, National Sun Yat-Sen University, Kaohsiung 804, Taiwan*

Mo Aqib Raza Khan − *Department of Marine Biotechnology, National Sun Yat-sen University, Kaohsiung 80424, Taiwan*

Chih-Chuang Liaw − *Department of Marine Biotechnology, National Sun Yat-sen University, Kaohsiung 80424, Taiwan*

Complete contact information is available at: https://pubs.acs.org/10.1021/acs.macromol.2c00417

Notes

The authors declare no competing financial interest.

ACKNOWLEDGMENTS

This study was supported financially by the Ministry of Science and Technology, Taiwan, under Contracts MOST 108-2638-E-002-003-MY2 and 108-2221-E-110-014-MY3. The authors also acknowledge the partial financial support from the National Natural Science Foundation of China (52073125).

REFERENCES

(1) Ishida, H.; Froimowicz, P. *Advanced and Emerging Polybenzoxazine Science and Technology*; Elsevier: Amsterdam, 2017.

(2) Machado, I.; Rachita, E.; Fuller, E.; Calado, V. M. A.; Ishida, H. Very High-Char-Yielding Elastomers Based on the Copolymers of a Catechol/Furfurylamine Benzoxazine and Polydimethylsiloxane Oligomers. *ACS Sustainable Chem. Eng.* **2021**, *9*, 16637−16650.

(3) Chong, A. M.; Salazar, S. A.; Stanzione, J. F., III Multifunctional Biobased Benzoxazines Blended with an Epoxy Resin for Tunable High-Performance Properties. *ACS Sustainable Chem. Eng.* **2021**, *9*, 5768−5775.

(4) Mohamed, M. G.; Kuo, S. W. Functional silica and carbon nanocomposites based on polybenzoxazines. *Macromol. Chem. Phys.* **2019**, *220*, 1800306.

(5) Wang, C. F.; Su, Y. C.; Kuo, S. W.; Huang, C. F.; Sheen, Y. C.; Chang, F. C. Low-surface-free-energy materials based on polybenzoxazines. *Angew. Chem., Int. Ed. Engl.* **2006**, *45*, 2248−2251.

(6) Mohamed, M. G.; Meng, T. S.; Kuo, S. W. Intrinsic water-soluble benzoxazine-functionalized cyclodextrin and its formation of inclusion complex with polymer. *Polymer* **2021**, *226*, 123827.

(7) Ohashi, S.; Rachita, E.; Baxley, S.; Zhou, J.; Erlichman, A.; Ishida, H. The first observation on polymerization of 1,3-benzothiazines:

synthesis of mono-and bis-thiazine monomers and thermal properties of their polymers. *Polym. Chem.* **2021**, *12*, 379−388.
(8) Mohamed, M. G.; Kuo, S. W. Crown ether-functionalized polybenzoxazine for metal ion adsorption. *Macromolecules* **2020**, *53*, 2420−2429.
(9) Fang, L.; Tao, Y.; Wang, C.; Dai, M.; Huang, G.; Sun, J.; Fang, Q. Resveratrol-Based Fluorinated Materials with High Thermostability and Good Dielectric Properties at High Frequency. *ACS Sustainable Chem. Eng.* **2020**, *8*, 16905−16911.
(10) Bayram, K.; Kiskan, B.; Yagci, Y. Synthesis of thioamide containing polybenzoxazines by the Willgerodt−Kindler reaction. *Polym. Chem.* **2021**, *12*, 534−544.
(11) Amarnath, N.; Shukla, S.; Lochab, B. Isomannide-Derived Chiral Rigid Fully Biobased Polybenzoxazines. *ACS Sustainable Chem. Eng.* **2019**, *7*, 18700−18710.
(12) Samy, M. M.; Mohamed, M. G.; Mansoure, T. H.; Meng, T. S.; Khan, M. A. R.; Liaw, C. C.; Kuo, S. W. Solid state chemical transformations through ring-opening polymerization of ferrocene-based conjugated microporous polymers in host−guest complexes with benzoxazine-linked cyclodextrin. *J. Taiwan Inst. Chem. Eng.* **2022**, *132*, 104110.
(13) Mohamed, M. G.; Chen, T. C.; Kuo, S. W. Solid-state chemical transformations to enhance gas capture in benzoxazine-linked conjugated microporous polymers. *Macromolecules* **2021**, *54*, 5866−5877.
(14) Wang, X.; Li, N.; Wang, J.; Li, G.; Zong, L.; Liu, C.; Jian, X. Hyperbranched polyether epoxy grafted graphene oxide for benzoxazine composites: enhancement of mechanical and thermal properties. *Compos. Sci. Technol.* **2018**, *155*, 11−21.
(15) Zhang, G.; EL-Mahdy, A. F. M.; Ahmed, L. R.; Matsagar, B. M.; Al-Saeedi, S.; Kuo, S. W.; Wu, K. C. W. Metal Complexes of the Porphyrin-Functionalized Polybenzoxazine. *Polymers* **2022**, *14*, 449.
(16) Samy, M. M.; Mohamed, M. G.; Kuo, S. W. Pyrene-functionalized tetraphenylethylene polybenzoxazine for dispersing single-walled carbon nanotubes and energy storage. *Compos. Sci. Technol.* **2020**, *199*, 108360.
(17) Adjaoud, A.; Puchot, L.; Verge, P. High-Tg and Degradable Isosorbide-Based Polybenzoxazine Vitrimer. *ACS Sustainable Chem. Eng.* **2022**, *10*, 594−602.
(18) Mohamed, M. G.; Samy, M. M.; Mansoure, T. H.; Li, C. J.; Li, W. C.; Chen, J. H.; Zhang, K.; Kuo, S. W. Microporous Carbon and Carbon/Metal Composite Materials Derived from Bio-Benzoxazine-Linked Precursor for CO_2 Capture and Energy Storage Applications. *Int. J. Mol. Sci.* **2022**, *23*, 347.
(19) Holly, F. W.; Cope, A. C. Condensation Products of Aldehydes and Ketones with o-Aminobenzyl Alcohol and o-Hydroxybenzylamine. *J. Am. Chem. Soc.* **1944**, *66*, 1875.
(20) Cai, W.; Wang, Z.; Shu, Z.; Liu, W.; Wang, J.; Qiu, J. Development of a fully bio-based hyperbranched benzoxazine. *Polym. Chem.* **2021**, *12*, 6894−6902.
(21) Zhang, X.; Mohamed, M. G.; Xin, Z.; Kuo, S. W. A tetraphenylethylene-functionalized benzoxazine and copper(II) acetylacetonate form a high-performance polybenzoxazine. *Polymer* **2020**, *201*, 122552.
(22) Mohamed, M. G.; Tsai, M. Y.; Su, W. C.; EL-Mahdy, A. F. M.; Wang, C. F.; Huang, C. F.; Dai, L.; Chen, T.; Kuo, S. W. Nitrogen-Doped microporous carbons derived from azobenzene and nitrile-functionalized polybenzoxazines for CO_2 uptake. *Mater. Today Commun.* **2020**, *24*, 101111.
(23) Yue, J.; He, L.; Zhao, P.; Gu, Y. Engineering Benzoxazine/Epoxy/Imidazole Blends with Controllable Microphase Structures for Toughness Improvement. *ACS Appl. Polym. Mater.* **2020**, *2*, 3458−3464.
(24) Liu, Y.; Sheng, W.; Yin, R.; Zhang, K. Propargylamine: an attractive amine source for designing high-performance benzoxazine resins with low polymerization temperatures. *Polym. Chem.* **2021**, *12*, 6694−6704.
(25) Adjaoud, A.; Trejo-Machin, A.; Puchot, L.; Verge, P. Polybenzoxazines: a sustainable platform for the design of fast responsive and catalyst-free vitrimers based on trans-esterification exchanges. *Polym. Chem.* **2021**, *12*, 3276−3289.
(26) Mohamed, M. G.; Kuo, S. W.; Mahdy, A.; Ghayd, A. I. M.; Aly, K. I. Bisbenzylidene cyclopentanone and cyclohexanone-functionalized polybenzoxazine nanocomposites: Synthesis, characterization, and use for corrosion protection on mild steel. *Mater. Today Commun.* **2020**, *25*, 101418.
(27) Kolanadiyil, S. N.; Minami, M.; Endo, T. Implementation of meta-Positioning in Tetrafunctional Benzoxazines: Synthesis, Properties, and Differences in the Polymerized Structure. *Macromolecules* **2020**, *53*, 6866−6886.
(28) Mukherjee, S.; Lochab, B. Synthesis and thermal behaviour of thiophene-based oxazine-ring substituted benzoxazine monomers & polymers. *Chem. Commun.* **2022**, *58*, 3609−3612.
(29) Alhwaige, A. A.; Ishida, H.; Qutubuddin, S. Poly(benzoxazine-f-chitosan) films: The role of aldehyde neighboring groups on chemical interaction of benzoxazine precursors with chitosan. *Carbohydr. Polym.* **2019**, *209*, 122−129.
(30) Samy, M. M.; Mohamed, M. G.; Kuo, S. W. Directly synthesized nitrogen-and-oxygen−doped microporous carbons derived from a bio-derived polybenzoxazine exhibiting high-performance supercapacitance and CO_2 uptake. *Eur. Polym. J.* **2020**, *138*, 109954.
(31) Aly, K. I.; Mahdy, A.; Hegazy, M. A.; Al-Muaikel, N. S.; Kuo, S. W.; Mohamed, M. G. Corrosion Resistance of Mild Steel Coated with Phthalimide-Functionalized Polybenzoxazines. *Coatings* **2020**, *10*, 1114.
(32) Mohamed, M. G.; Ebrahium, S. M.; Hammam, A. S.; Kuo, S. W.; Aly, K. I. Enhanced CO_2 capture in nitrogen-enriched microporous carbons derived from Polybenzoxazines containing azobenzene and carboxylic acid units. *J. Polym. Res.* **2020**, *27*, 197.
(33) Aly, K. I.; Mohamed, M. G.; Younis, O.; Mahross, M. H.; Hakim, M. A.; Sayed, M. M. Salicylaldehyde azine-functionalized polybenzoxazine: Synthesis, characterization, and its nanocomposites as coatings for inhibiting the mild steel corrosion. *Prog. Org. Coat.* **2020**, *138* (12020), 105385.
(34) Wang, T. C.; Tsai, C. Y.; Liu, Y. L. Solid Polymer Electrolytes Based on Cross-Linked Polybenzoxazine Possessing Poly(ethylene oxide) Segments Enhancing Cycling Performance of Lithium Metal Batteries. *ACS Sustainable Chem. Eng.* **2021**, *9*, 6274−6283.
(35) Wu, J. Y.; Mohamed, M. G.; Kuo, S. W. Directly synthesized nitrogen-doped microporous carbons from polybenzoxazine resins for carbon dioxide capture. *Polym. Chem.* **2017**, *8*, 5481−5489.
(36) Sha, X. L.; Yuan, L.; Liang, G.; Gu, A. Heat-resistant and robust biobased benzoxazine resins developed with a green synthesis strategy. *Polym. Chem.* **2021**, *12*, 432−438.
(37) Abuzeid, H. R.; EL-Mahdy, A. F. M.; Ahmed, M. M. M.; Kuo, S. W. Triazine-functionalized covalent benzoxazine framework for direct synthesis of N-doped microporous carbon. *Polym. Chem.* **2019**, *10*, 6010−6020.
(38) Hong, L.; Ju, S.; Liu, X.; Zhuang, Q.; Zhan, G.; Yu, X. Highly Selective CO_2 Uptake in Novel Fishnet-like Polybenzoxazine-Based Porous Carbon. *Energy Fuels* **2019**, *33*, 11454−11464.
(39) Mohamed, M. G.; Atayde, E. C.; Matsagar, B. M.; Na, J.; Yamauchi, Y.; Wu, K. C.-W.; Kuo, S. W. Construction Hierarchically Mesoporous/Microporous Materials Based on Block Copolymer and Covalent Organic Framework. *J. Taiwan Inst. Chem. Eng.* **2020**, *112*, 180−192.
(40) Shi, W.; Zhang, X.; Ji, Y.; Zhao, Z.; Li, W.; Jia, X. Sustainable Preparation of Bio-Based Polybenzoxazine Resins from Amino Acid and Their Application in CO_2 Adsorption. *ACS Sustainable Chem. Eng.* **2019**, *7*, 17313−17324.
(41) Liu, Y.; Cao, L.; Luo, J.; Peng, Y.; Ji, Q.; Dai, J.; Zhu, J.; Liu, X. Biobased Nitrogen- and Oxygen-Codoped Carbon Materials for High-Performance Supercapacitor. *ACS Sustainable Chem. Eng.* **2019**, *7*, 2763−2773.
(42) Deng, Y.; Xia, L.; Song, G. L.; Zhao, Y.; Zhang, Y.; Xu, Y.; Zheng, D. Development of a curcumin-based antifouling and anticorrosion sustainable polybenzoxazine resin composite coating. *Compos. B. Eng.* **2021**, *225*, 109263.

https://doi.org/10.1021/acs.macromol.2c00417
Macromolecules 2022, 55, 3106−3115

(43) Sha, X. L.; Yuan, L.; Liang, G.; Gu, A. Development and Mechanism of High-Performance Fully Biobased Shape Memory Benzoxazine Resins with a Green Strategy. *ACS Sustainable Chem. Eng.* **2020**, *8*, 18696−18705.
(44) Arslan, M.; Kiskan, B.; Yagci, Y. Recycling and Self-Healing of Polybenzoxazines with Dynamic Sulfide Linkages. *Sci. Rep.* **2017**, *7*, 5207.
(45) Arslan, M.; Kiskan, B.; Yagci, Y. Benzoxazine-Based Thermoset with Autonomous Self-Healing and Shape Recovery. *Macromolecules* **2018**, *51*, 10095−10103.
(46) Salum, M. L.; Iguchi, D.; Arza, C. R.; Han, L.; Ishida, H.; Froimowicz, P. Making Benzoxazines Greener: Design, Synthesis, and Polymerization of a Biobased Benzoxazine Fulfilling Two Principles of Green Chemistry. *ACS Sustainable Chem. Eng.* **2018**, *6*, 13096−13106.
(47) Ručigaj, A.; Ambrožič, R.; Krajnc, M. Thermally Assisted Self-Healing and Shape Memory Behavior of Diphenolic Acid-Based Benzoxazines. *Macromol. Mater. Eng.* **2020**, *305*, 2000463.
(48) Zhang, K.; Han, M.; Liu, Y.; Froimowicz, P. Design and Synthesis of Bio-Based High-Performance Trioxazine Benzoxazine Resin via Natural Renewable Resources. *ACS Sustainable Chem. Eng.* **2019**, *7*, 9399−9407.
(49) Sini, N. K.; Bijwe, J.; Varma, I. K. Renewable benzoxazine monomer from Vanillin: Synthesis, characterization, and studies on curing behavior. *J. Polym. Sci., Part A: Polym. Chem.* **2014**, *52*, 7−11.
(50) Kotzebue, L. R. V.; De Oliveira, J. R.; Da Silva, J. B.; Mazzetto, S. E.; Ishida, H.; Lomonaco, D. Development of Fully Biobased High-Performance Bis-Benzoxazine under Environmentally Friendly Conditions. *ACS Sustainable Chem. Eng.* **2018**, *6*, 5485−5494.
(51) Monisha, M.; Yadav, N.; Lochab, B. Sustainable Framework of Chitosan−Benzoxazine with Mutual Benefits: Low Curing Temperature and Improved Thermal and Mechanical Properties. *ACS Sustainable Chem. Eng.* **2019**, *7*, 4473−4485.
(52) Omura, Y.; Taruno, Y.; Irisa, Y.; Morimoto, M.; Saimoto, H.; Shigemasa, Y. Regioselective Mannich reaction of phenolic compounds and its application to the synthesis of new chitosan derivatives. *Tetrahedron Lett.* **2001**, *42*, 7273−7275.
(53) Alhwaige, A. A.; Agag, T.; Ishida, H.; Qutubuddin, S. Biobased Chitosan/Polybenzoxazine Cross-Linked Films: Preparation in Aqueous Media and Synergistic Improvements in Thermal and Mechanical Properties. *Biomacromolecules* **2013**, *14*, 1806−1815.
(54) Dai, J.; Teng, N.; Peng, Y.; Liu, Y.; Cao, L.; Zhu, J.; Liu, X. Biobased Benzoxazine Derived from Daidzein and Furfurylamine: Microwave-Assisted Synthesis and Thermal Properties Investigation. *ChemSusChem* **2018**, *11*, 3175−3183.
(55) Han, M.; You, S.; Wang, Y.; Zhang, K.; Yang, S. Synthesis of Highly Thermally Stable Daidzein-Based Main-Chain-Type Benzoxazine Resins. *Polymers* **2019**, *11*, 1341.
(56) Yan, X.; Qi, M.; Li, P.; Zhan, Y.; Shao, H. Apigenin in cancer therapy: anti-cancer effects and mechanisms of action. *Cell Biosci.* **2017**, *7*, 50.
(57) Zhang, J.; Liu, D.; Huang, Y.; Gao, Y.; Qian, S. Biopharmaceutics classification and intestinal absorption study of apigenin. *Int. J. Pharmaceut.* **2012**, *436*, 311−317.
(58) Zhang, K.; Liu, Y.; Han, M.; Froimowicz, P. Smart and sustainable design of latent catalyst-containing benzoxazine-bio-resins and application studies. *Green Chem.* **2020**, *22*, 1209−1219.
(59) Hao, B.; Han, L.; Liu, Y.; Zhang, K. An apigenin-based bio-benzoxazine with three polymerizable functionalities: sustainable synthesis, thermal latent polymerization, and excellent thermal properties of its thermosets. *Polym. Chem.* **2020**, *11*, 5800−5809.
(60) Mukherjee, S.; Amarnath, N.; Lochab, B. Oxazine Ring-Substituted 4th Generation Benzoxazine Monomers & Polymers: Stereo electronic Effect of Phenyl Substituents on Thermal Properties. *Macromolecules* **2021**, *54*, 10001−10016.
(61) Machado, I.; Hsieh, I.; Rachita, E.; Salum, M. L.; Iguchi, D.; Pogharian, N.; Pellot, A.; Froimowicz, P.; Calado, V.; Ishida, H. A truly bio-based benzoxazine derived from three natural reactants obtained under environmentally friendly conditions and its polymer properties. *Green Chem.* **2021**, *23*, 4051−4064.
(62) Tavernier, R.; Granado, L.; Foyer, G.; David, G.; Caillol, S. Formaldehyde-Free Polybenzoxazines for High Performance Thermosets. *Macromolecules* **2020**, *53*, 2557−2567.
(63) Wang, H.; Wang, J.; He, X.; Feng, T.; Ramdani, N.; Luan, M.; Liu, W.; Xu, X. Synthesis of novel furan-containing tetrafunctional fluorene-based benzoxazine monomer and its high-performance thermoset. *RSC Adv.* **2014**, *4*, 64798−64801.
(64) Kissinger, H. E. Reaction Kinetics in Differential Thermal Analysis. *Anal. Chem.* **1957**, *29*, 1702−1706.
(65) Ozawa, T. Kinetics of non-isothermal crystallization. *Polymer* **1971**, *12*, 150−158.
(66) Zhang, K.; Ishida, H. An anomalous trade-off effect on the properties of smart ortho-functional benzoxazines. *Polym. Chem.* **2015**, *6*, 2541−2550.
(67) Tsibouklis, J.; Stone, M.; Thorpe, A. A.; Graham, P.; Nevell, T. G.; Ewen, R. J. Surface energy characteristics of polymer film Structures: A further insight into the molecular design requirements. *Langmuir* **1999**, *15*, 7076−7079.
(68) Owens, D. K.; Wendt, R. C. Estimation of the surface free energy of polymers. *J. Appl. Polym. Sci.* **1969**, *13*, 1741−1747.
(69) Khan, M. A. R.; Wang, B. W.; Chen, Y. Y.; Lin, T. H.; Lin, H. C.; Yang, Y. L.; Pang, K. L.; Liaw, C. C. Natural polyketide 6-pentyl-2 H-pyrone-2-one and its synthetic analogues efficiently prevent marine biofouling. *Biofouling.* **2021**, *37*, 257−266.
(70) Liaw, C. C.; Chen, P. C.; Shih, C. J.; Tseng, S. P.; Lai, Y. M.; Hsu, C. H.; Dorrestein, P. C.; Yang, Y. L. Vitroprocines, new antibiotics against Acinetobacter baumannii, discovered from marine Vibrio sp. QWI-06 using mass-spectrometry-based metabolomics approach. *Sci. Rep.* **2015**, *5*, 12856.

https://doi.org/10.1021/acs.macromol.2c00417
Macromolecules 2022, 55, 3106−3115